

Halogenated Diazirines as Photolabel Mimics of the Inhaled Haloalkane Anesthetics

Roderic G. Eckenhoff,^{*,†} Frank J. Knoll,[‡] Eric P. Greenblatt,[†] and William P. Dailey[‡]

Department of Anesthesia, University of Pennsylvania Health System, 3400 Spruce Street, Philadelphia, Pennsylvania 19104-4283, and Department of Chemistry, School of Arts and Sciences, University of Pennsylvania, Philadelphia, Pennsylvania 19104

Received October 23, 2001

The inhaled anesthetics are low affinity volatile compounds whose mechanism of action remains unclear, in part due to the difficulty of determining their binding targets. Photolabeling may help resolve this difficulty, and thus we have synthesized six compounds (four previously unreported) with structural and physical similarity to halothane (1-bromo-1-chloro-2,2,2-trifluoroethane), a commonly used clinical anesthetic. These compounds incorporate either a diazo, diazirine, or azido group to provide photolability in the long-UV range and to provide a highly reactive photolysis product. While several of the compounds have immobilizing activity in tadpoles, it is complicated by either toxicity or very low potency. One compound however, a halogenated three-carbon diazirine **4**, is a potent anesthetic, is apparently nontoxic, potentiates GABA_A Cl⁻ currents, and stabilizes serum albumin, all of which are features of halothane. When tagged with radioactivity, this compound should serve as a reasonable probe of haloalkane anesthetic binding targets and sites.

Introduction

Characterizing the molecular targets of the inhaled anesthetics has been hampered by the low apparent affinity for these clinically important drugs.¹ Low affinity is suggested by high clinical EC₅₀ values (~0.3 mM) and also the fact that dissociation constants lower than about 0.5 mM have not yet been described for any target. Such weak binding interactions translate to very brief occupancy of binding sites, making conventional radioligand binding studies impossible. Alternative methods for characterizing binding have been introduced, but all suffer from limitations. For example, tryptophan fluorescence quenching requires a tryptophan residue in the binding site, which exists in some proteins,² but not others.^{3,4} Further, the anesthetic ligand must contain a heavy atom to produce contact quenching, and it must bind in an orientation that brings the heavy atom to within about 5 Å of the indole moiety of the tryptophan. Too many tryptophan residues make interpretation difficult, but fortunately, these are relatively rare residues in most proteins.¹⁹F NMR,⁵ isothermal titration calorimetry,⁶ and amide hydrogen exchange⁷ can each detect anesthetic binding in purified proteins, but suffer from an inability to provide spatial information, and cannot identify targets from complex mixtures.

To provide ligand contact sites along the primary sequence in individual targets and to allow selection of targets from complex mixtures (e.g., biological membranes), we introduced direct photolabeling for the well-

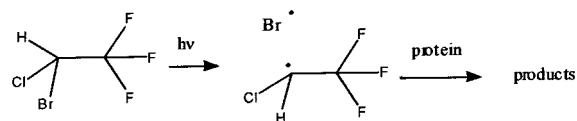


Figure 1. Photochemical reaction of halothane with a protein. This reaction requires short UV light (200–250 nm) and releases two reactive products: chlorotrifluoroethyl radical and a free bromine atom.

known inhaled anesthetic halothane (1-bromo-1-chloro-2,2,2-trifluoroethane), almost a decade ago.⁸ In this case, the C–Br bond of halothane is cleaved by 250 nm light, yielding two reactive products, a chlorotrifluoroethyl radical and a free bromine atom (Figure 1). Both products can react with target sites in what could be complex photochemistry, but we have found that the carbon-centered radical becomes covalently incorporated in a reproducible and conformationally sensitive manner,^{8,9} strongly suggesting that it reliably reports halothane equilibrium binding sites. Combined with autoradiography, halothane photolabeling has also allowed mapping of the distribution¹⁰ and pharmacology¹¹ of halothane binding in the mammalian brain. Nevertheless, the relatively long-lived radical (~1 μs) could allow it to diffuse to sites of preferential photoreactivity, possibly blurring residue-level resolution. More importantly, the 250 nm radiation is damaging to molecular targets, making the subsequent biochemical analyses of labeled material difficult.

We have therefore undertaken an effort to produce an improved volatile anesthetic photolabel. We chose to incorporate the diazo- or diazirine group into two- and three-carbon haloalkanes, since this group undergoes photolysis at ~350 nm, an essentially nondamaging range of UV light, and because only a single reactive moiety results. The photolysis reaction for such compounds is shown in Figure 2. The reactive product from

* Correspondence: Roderic G. Eckenhoff, MD, 780 Dulles Bldg, HUP, 3400 Spruce Street, Philadelphia, PA 19104-4283. Fax: 215-349-5078. Voice: 215-662-3705. E-mail: roderic.eckenhoff@uphs.upenn.edu.

[†] Department of Anesthesia, University of Pennsylvania Health System.

[‡] Department of Chemistry, University of Pennsylvania.

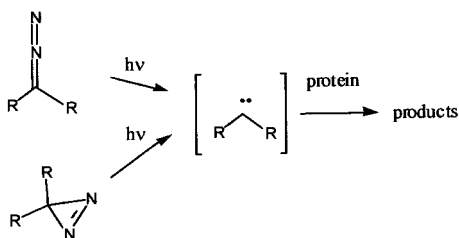


Figure 2. Reaction of a diazo- or diazirine-containing compound with a protein. This reaction requires long UV (300–400 nm) and requires a single highly reactive carbene product.

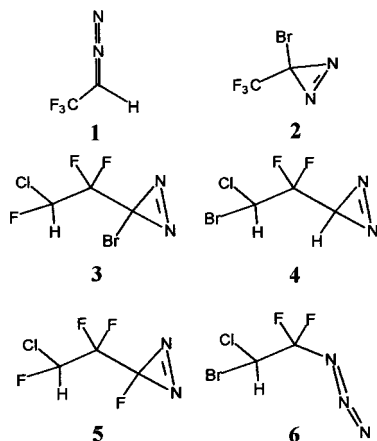


Figure 3. Compounds synthesized for study in this investigation.

either diazo or diazirine photolysis is a carbene,¹² which has a lifetime several orders of magnitude shorter than the carbon-centered radical product of halothane photolysis. In addition, unlike the radical, the carbene can insert into almost any chemical bond, including C–C or C–H bonds. This considerably reduces the likelihood that photochemical selectivity will contaminate the labeling pattern. When suitable compounds are produced, ¹⁴C or ³H atoms can be included during or after synthesis to allow monitoring of adduction.

Despite the drawbacks cited above, halothane has the enormous advantage of being an anesthetic with a 50 year history of clinical application and laboratory study. Any new photolabel proposed as an anesthetic mimic must therefore satisfy as many existing criteria for a general inhalational anesthetic as possible. Thus, in this study, we examine octanol solubility, specific binding to serum albumin,^{2,5,8,13} potentiation of GABA-gated chloride currents,^{14,15} and finally, reversible immobility in tadpoles, a well-established animal model for testing anesthetics. We fully anticipate that these compounds will display toxicity in intact animals unlike our general anesthetics, by virtue of the cyanide-like diazo, diazirine, or azido groups. This toxicity ought to be distinguishable from anesthetic-like activity from the time-course and recovery profile. For example, anesthetic activity should occur rapidly and be reversible, while toxicity is expected to be progressive and irreversible. Our efforts so far have produced six compounds, **1–6**, shown below (Figure 3). Compounds **1** and **2** were previously reported while the remaining compounds were synthesized for this study. Compounds **1–5** are potential photochemical precursors to carbenes. Compound **6** is a potential photochemical precursor to a nitrene, the nitrogen analogue of a carbene. It should

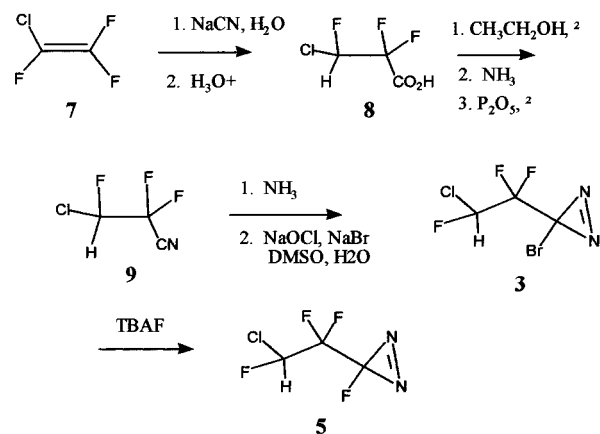
be noted, however, that most of these compounds are also somewhat unstable and can explode with considerable force if subjected to shock, spark, or even phase changes. Because of this, and synthetic difficulties, it is important to note that only small amounts of these compounds ($\ll 1$ g) were produced at any one time.

Results

Synthesis of Compounds 1–6. Compounds **1**¹⁶ and **2**¹⁷ have been previously reported in the literature and were prepared according to previous methods. Compounds **3–6** have not previously been reported.

The preparation of **3** and **5** is shown in Scheme 1. Treatment of commercially available chlorotrifluoroethene with sodium cyanide in aqueous acetonitrile produced the carboxylic acid **8** in good yield.¹⁸ Esterification, amidation, and dehydration produced the known nitrile **9**.¹⁹ Condensation of nitrile **9** with ammonia followed by Graham oxidation²⁰ of the crude amidine produced the bromo diazirine **3**. Use of the fluoride exchange²¹ reaction led to the production of **5**.

Scheme 1



Preparation of **4** (Scheme 2) started with reduction of 1-bromo-1-chloro-2,2,2-trifluoroethane (halothane, **10**) using zinc dust to yield chlorodifluoroethene (**11**).²²

Scheme 2

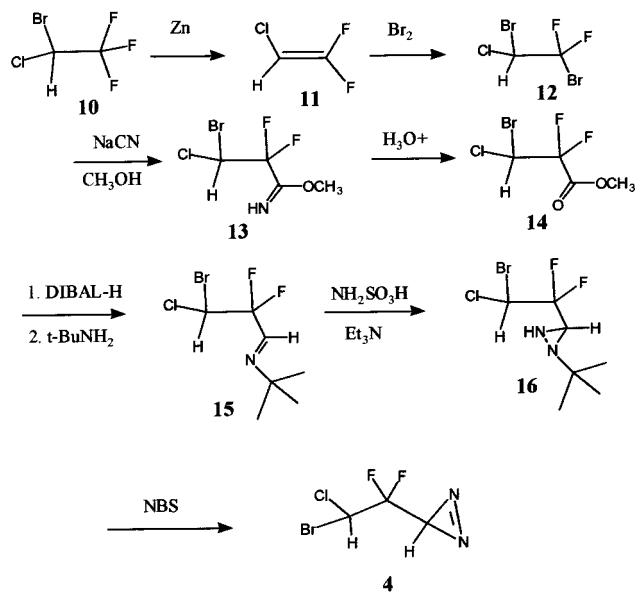


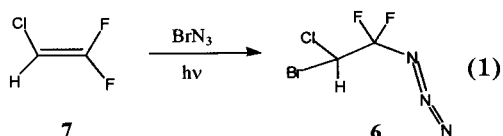
Table 1. Physical Properties

compd	MW	boiling pt ^a	extinction ^b @ nm	dipole, D ^c	octanol: water ^d
1	110	11	20 @ 400 nm	2.1	40
2	189	-30	70 @ 335 nm	0.6	>500
3	238	80	70 @ 338 nm	1.1	150
4	212	102	160 @ 312 nm	2.8	80
5	177	25	70 @ 327 nm	1.5	
6	219	123	1540 @ 204 nm	2.3	210
halothane	198	58	410 @ 208 nm	1.4	180

^a Zubrick, J. W. *The Organic Chem Lab Survival Manual*, 4th ed; Wiley: New York, pp 247–249. ^b Molar coefficient. ^c Calculated using ab initio theory using full geometry optimization at the HF/6-311+(2d,p) level using Gaussian 94. ^d Based on repetitive measurements of halothane octanol:water coefficient. The precision of our method is $\pm 10\%$.

Alkene **11** was immediately converted to dibromide **12** which was treated with sodium cyanide in methanol to give imidate **13**. Careful hydrolysis produced ester **14** which was treated with DIBAL-H to give the aldehyde as a mixture of hydrate and hemiacetal. This crude mixture was converted directly to imine **15** using *tert*-butylamine under reflux in toluene. Conversion of imine **15** to diaziridine **16** followed established protocols²³ using reaction of hydroylaminesulfonic acid and triethylamine. Oxidation of diaziridine **16** to diazirine **4** was problematic. Good yields of relatively pure material finally were prepared by using *N*-bromosuccinimide as the oxidizing reagent. The other volatile produce, *tert*-butylbromide, could be separated by careful distillation followed by preparative GC.

The preparation of **6** made use of the photochemically induced radical addition of bromine azide to **7** using a modification of the general procedure of Hassner et al.²⁴ (eq 1).



Electronic Structure Calculations. As an aid in the characterization of compounds **1–6**, ab initio molecular orbital calculations were carried out on these structures using the Gaussian94 program.²⁵ It was recently reported that large basis sets are needed to accurately reproduce the dipole moment of halothane.²⁶ Thus a similar basis set (6-311+ 2d,p) along with complete geometry optimization was used to determine the structures and dipole moments of compounds **1–6**. The calculated dipole moments are listed in Table 1.

Biological Evaluation of Compounds 1–6. (i) Tadpole Immobility. Compounds **1** and **2** produced only a modest decrease in tadpole mobility in the 5 min exposure, even at the highest concentrations achieved in pond water. However, both compounds were clearly toxic, with significant mortality after even short exposures. Thus, immobility due to reversible as compared to irreversible effects of these compounds was a difficult distinction. Compound **3** slowly produced tadpole immobility with an EC₅₀ of about 0.3 mM after 5 min, with clear but slow recovery. Significant mortality occurred several hours later. Compound **4** produced rapid onset of reversible immobility with an EC₅₀ of about 0.1 mM. Recovery was complete with no evidence of toxicity after

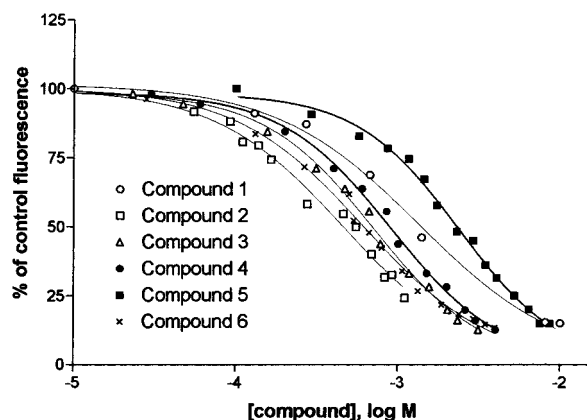


Figure 4. Intrinsic fluorescence quenching by the various compounds. Increasing concentrations of each compound are plotted against fluorescence maxima of HSA (corrected for inner-filtering). All the compounds effectively quench the fluorescence of this protein, with **2** and **6** being the most potent, and **1** and **5** the least.

24 h, even when the tadpoles were exposed to $10 \times$ EC₅₀ concentrations (this was also true of halothane, although recovery was faster with halothane). Compound **5** was considerably less potent than **4**, with an EC₅₀ of about 2.5 mM, but was also devoid of toxicity. Finally, **6** rapidly immobilized the tadpoles even at low (~ 0.5 mM) concentration, but without any signs of reversibility. Complete long term (24 h) mortality occurred even with brief, subimmobilizing exposures to compound **6** concentrations (~ 0.1 mM).

(ii) Physicochemical Properties. The difficult syntheses and resultant small volumes of the prepared compounds precluded precise, repetitive measurements of the physical properties. Thus, the properties of **1–6** shown in Table 1 should be considered estimates or, in the case of the dipole moment, calculations. All compounds are relatively hydrophobic and have dipole moments less than 3 D. Most of these compounds absorbed light in the 300–350 nm range, but **6** only had detectable absorbance below 280 nm. Boiling points below room temperature made for difficult handling and measurement of **1** and **2** in the biologic experiments. None of these physical parameters correlated well with the sedating/anesthetizing behavior in tadpoles.

(iii) Fluorescence Quenching in HSA. Similar to inhaled anesthetics, **1–6** bound to the tryptophan-containing region of HSA as indicated by tryptophan fluorescence quenching. Figure 4 shows that each compound quenched greater than 80% of trp-214 fluorescence, with EC₅₀ values ranging from 0.4 to 2.2 mM and Hill slopes between 1 and 1.5 (Table 3). Compounds **2**, **3**, **4**, and **6** (Br-containing) were most potent and fairly similar, and **1** and **5** (no Br) were least potent.

(iv) Hydrogen Exchange. All of the compounds stabilized BSA against unfolding as reflected by a slowed rate of hydrogen exchange. As shown in Table 2, the rank order for stabilization was **4** > **6** > **1** > **3** > **5** > **2**. However, because concentrations of the various compounds in the exchange out buffer were different for each experiment, we used the following equation to estimate a dissociation constant to provide some normalization:

$$\text{PFR} = 1 + ([\text{compound}]/K_D)^n$$

Table 2. BSA Stabilization

compd, concd	PFr ^a	$\Delta\Delta G$, kcal/mol	K_D , mM
1, 5 mM	4.8	1.0	1.3
2, 2.5 mM	1.5	0.2	5.6
3, 1.4 mM	3.5	0.8	0.6
4, 3.4 mM	22.9	1.9	0.2
5, 7.0 mM	2.5	0.6	4.8
6, 2.0 mM	8.4	1.3	0.3
halothane, 6 mM	6.6	1.2	0.9

^a PFr values are derived from several groups of hydrogens and are reproducible to about 5% between experiments, rendering the derived K_D and $\Delta\Delta G$ values similarly precise. Measurements of the halothane/BSA K_D using other methods (2, 5), are very consistent with this HX approach (~1 mM).

Table 3. HSA Fluorescence Quenching

compd	IC ₅₀ (95% C.I.), mM	Hill slope (95% C.I.)
1	1.2 (1.0–1.5)	–1.1 (–1.3 to –0.9)
2	0.4 (0.3–0.5)	–1.2 (–1.4 to –0.9)
3	0.7 (0.6–0.7)	–1.4 (11.6 to –1.2)
4	0.8 (0.8–0.9)	–1.5 (–1.6 to –1.2)
5	2.2 (2.0–2.4)	–1.5 (–1.7 to –1.3)
6	0.3 (0.2–0.3)	–1.2 (–1.3 to –1.1)
halothane	2.9 (2.8–3.1)	–1.5 (–1.6 to –1.5)

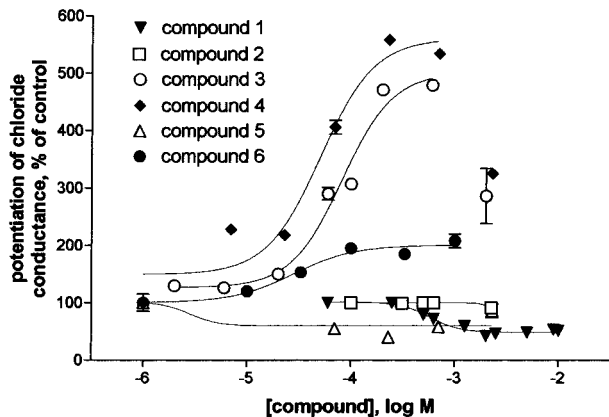


Figure 5. Effect of each compound on chloride channel conductance of GABA receptors expressed in *xenopus* oocytes. All these experiments were performed in the presence of an EC₁₀ concentration of GABA (~10 μ M, but slightly different for each oocyte). Compounds 3 and 4 potentiated conductance the most, 6 was intermediate, and 1, 2, and 5 did not potentiate at all.

where PFr is the hydrogen protection factor ratio (compound/control), and n = number of binding sites.⁹ For simplicity, we assumed a single binding site, and derived the following rank order for K_D : 4 > 6 > 3 > 1 > 5 > 2, which is approximately similar to the crude stabilization $\Delta\Delta G$ rank. Interestingly, halothane is intermediate (between compounds 6 and 3) in potency for BSA stabilization.

(v) GABA_A Receptor Studies. As shown in Figure 5, the compounds separated into two groups in these experiments. Compounds 3, 4, and 6 resulted in significant potentiation of GABA responses, while all the others either had no effect or produced slight inhibition of GABA responses. Compound 4 was the most potent with an EC₅₀ of about 50 μ M and that for compound 3 was about 80 μ M. Like other inhaled anesthetics, none of the compounds directly gated these channels, and at high compound concentration, the GABA response was less potentiated (“drop-off”). Compound 6 showed only a ~2-fold enhancement of GABA Cl[–] currents and no

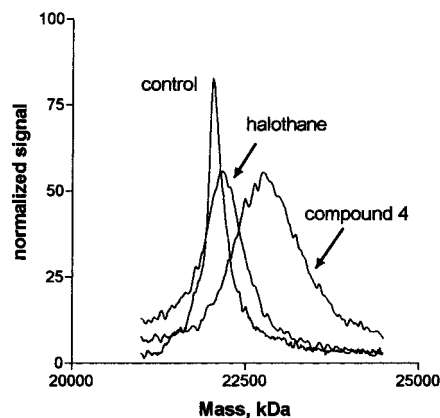


Figure 6. Exposure of an HSA domain II peptide to 4 or halothane and UV light (300 and 254 nm, respectively) produced an increase in MW as shown on MALDI-MS.

evidence of drop off. All of these effects were fully reversible on washout, although prolonged washout (15 min) was required with 6 and at the higher concentrations of most of the other compounds.

(vi) Photolabeling. Of this group, compound 4 appeared to show the most promise as a general anesthetic mimic, so photolabeling to HSA domain II was carried out only with this compound. On MALDI analysis (Figure 6), the unlabeled HSA domain II had a mass peak at 22034 Da, and this was significantly increased to 22737 in the presence of 2 mM 4 and 300 nm light, indicating a mean incorporation stoichiometry of 3.7:1. For comparison, the same peptide with halothane and 254 nm illumination resulted in a mass of 22159 Da, or an incorporation stoichiometry of about 1:1. Exposure of the peptide to UV without the compound broadened the peak somewhat but had no effect on the centroid position (data not shown).

Discussion

Only one of the six compounds showed significant similarity to inhaled anesthetics such as halothane. Compound 4 had a rapid onset of action, a more prolonged action than halothane, but complete recovery and no signs of toxicity in the 24 h of observation. It is slightly more potent than halothane. While it is still possible for there to be delayed toxicity due to metabolism of this compound, the acute pharmacological profile seems very similar to the clinically used inhaled anesthetics. Compound 3 also had anesthetic-like activity, but the rapid development of toxicity made the anesthetic potency difficult to evaluate. Compound 6 may have had anesthetic activity but was also the most toxic of the group, so measurement of potency was ambiguous. Compounds 1, 2, and 5 had little acute immobilizing effect, primarily a progressively slow effect more likely due to toxicity as opposed to anesthesia or sedation.

There appears to be little structural correlation with anesthetic potency, as is also true for the many clinically used compounds. Compound 4 has the bromochlorodifluoroethyl moiety shared by halothane, but so does 6. It is, of course, possible that both are potent anesthetics but that the azido group on 6 is so acutely toxic that it masks any anesthetic potency. A similar chlorofluorodifluoroethyl group (3 and 5) appear to only weakly confer

anesthetic activity, and neither of the two carbon molecules (**1** and **2**) had significant activity. Similarly, physical properties did not correlate well with reversible immobilizing activity in tadpoles, although many more compounds would be required for a valid analysis. The physical properties of **3** appear to be most like those of halothane, but it possessed only marginal immobilizing activity. Compound **4** had a considerably larger calculated dipole and lower octanol:water solubility than halothane but was more potent—an opposite prediction of the Overton–Meyer correlation. Thus, it would appear that inclusion of these photoreactive groups alters the molecular features of these small molecules enough to disrupt the simple relationship between hydrophobicity and potency or that they introduce a second biologic activity which masks or obviates the other in an intact organism.

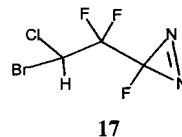
Fluorescence Quenching. HSA was used for these studies because it has a single tryptophan residue, whereas BSA has two. Thus, HSA allows a direct comparison of quenching efficacy at the same site, while BSA would be ambiguous. All of the compounds were able to quench HSA fluorescence and in a fairly similar concentration range. This indicates that the interdomain cavity containing the tryptophan in HSA is not sufficiently selective to distinguish between these different compounds, which clearly were distinguished by the other assays. This is consistent with previous work, in that stereoisomers of isoflurane could not be distinguished by fluorescence quenching (data not shown) but could by other measures of binding in this same protein.¹⁵ Other measures of the tryptophan environment, such as anisotropy, might be more sensitive to subtleties of ligand structure than quenching.

BSA Stabilization. As compared to fluorescence quenching, there was a fairly good correlation between stabilization of the entire albumin molecule and anesthetic activity as indicated by tadpole behavior. This is presumably more sensitive than fluorescence quenching because global stability is a function of occupancy of many binding sites of different character and therefore has a greater chance of reflecting relevant *in vivo* targets. Thus, **4** was the most efficient stabilizer, with an estimated global K_D of 0.16 mM assuming only one site. Again, the other molecule containing the bromochlorodifluoro group (**6**) was also a potent stabilizer, with a K_D of 0.27 mM, suggesting that its rapid immobilizing activity may indeed be an anesthetic effect, closely followed by toxicity. The next most potent stabilizer was **3**, also a compound with some sedative properties. These K_D estimates are an overestimation, because other evidence clearly shows multiple binding sites on BSA. But because the number of sites is likely to be similar, the relative difference between the compounds should be preserved.

GABA_A Potentiation. Interestingly, the ability to potentiate GABA_A channels in xenopus oocytes grouped the compounds into two clear classes—those that potentiated and those that did nothing (or inhibited slightly). Compounds **3** and **4** are clearly similar to halothane and other inhaled anesthetics in an ability to potentiate Cl⁻ conductance at low [GABA], an inability to gate directly, and evidence of drop-off at high concentration. These two compounds also showed the

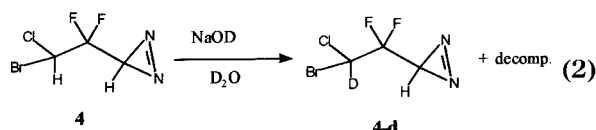
most convincing immobilizing activity in tadpoles and were potent stabilizers of BSA. Compound **6** also potentiated GABA-mediated Cl⁻ conductance, with potency similar to that of **3** and **4** but with significantly less efficacy. This is unlikely to be related to parallel toxicity in this oocyte system since the effects were fully reversible. Thus, it would appear that, at least in this one assay, **6** is less like an anesthetic than either **3** or **4**.

Promise as a Photolabel. Thus, in summary, compound **4** appears to meet many of the criteria of an anesthetic mimic. Further, we verified an ability to adduct to a known binding protein, with a realistic stoichiometry. The fact that halothane binding stoichiometry was 3-fold lower is probably due to the shorter illumination time and the fact that we did not remove molecular oxygen from the buffer in this experiment (oxygen is a known scavenger of the carbon-centered radical and therefore competes for binding to targets). Compound **4** shows an absorption peak at around 310 nm, which although considerably better than halothane at 210 nm, is still close to some of the absorption peaks of proteins—particularly the aromatic residues. We believe that compound **17** which incorporates a fluorine on the diazirine carbon, instead of the hydrogen, will have several beneficial features. First, it should



enhance the volatility closer to that of halothane. Second, the peak absorption of the diazirine group should be red-shifted, making it more remote from that of proteins. Third, because both **3** and **4** had anesthetic activity, we are confident that this fluorine analogue of **4** will retain anesthetic properties. Attempts to prepare **17** are currently underway.

Combined with the above results, this shows that a suitable photolabel mimic, with improved properties over halothane, has been synthesized and could be employed as a probe for identifying anesthetic binding targets and sites. This will require the incorporation of a labeled group of some sort to track adduction, select preferential targets from a complex mixture, and uncover primary sequence binding sites from microsequence analysis. Radiolabels are most commonly used because of the extreme detection sensitivity, and also the ability to determine specificity of binding by competition with unlabeled ligand. The most logical form of tagging in this case would be an exchange tritiation with the acidic hydrogen atom on **4**. Preliminary experiments have shown that the analogous deuteration can be achieved (eq 2), but there is competitive decomposition of the molecule. Adduction to proteins could also be monitored with mass spectroscopy, in both the intact protein and proteolytic fragments, but this loses the ability to detect specificity and is also less sensitive than radioactive tags. Finally, photolabeling can be detected by virtue of other elements on the adduct—such as the fluorine. It should be possible to use ¹⁹F NMR to detect fluorine in purified peptides and perhaps also in gel or column separated fractions.



In summary, we have developed a photolabile molecule that behaves like an inhaled anesthetic in several *in vitro* assays and should serve as a scaffold for further development of the ideal inhaled anesthetic photoaffinity probe.

Experimental Section

Materials. ^3HOH was obtained from Amersham. HSA domain II was a kind gift of Dr. R. Bhagavan, University of Hawaii). All other chemicals were of reagents grade or better and were obtained from Sigma or Aldrich. Trifluoromethyl-diazomethane¹⁶ (**1**) and 3-bromo-3-trifluoromethyl-3*H*-diazirine¹⁷ (**2**) were prepared according to the published methods. CAUTION: All diazirines and diazo compounds are potentially explosive and should be treated with due care. All new compounds exhibited IR and high-resolution mass spectra consistent with the assigned structures. Final products **1**, **2**, **3**, **4**, **5**, and **6** were purified by preparative gas chromatography (GC) using a 1/4 in. \times 10 ft 10% SF-96 on Chromasorb W support with a column temperature between ambient and 50 °C depending on the compound and with the injection and detector ports 25 °C higher than the column. The final purified compounds were >98% pure by GC analysis using a 30 m dimethylsilicone capillary column and flame ionization detection using 50 °C column temperature and on-column injection at 75 °C.

Preparation of 3-Bromo-3-(2-chloro-1,1,2-trifluoroethyl)-3*H*-diazirine (3**).** A two-necked 25 mL rb flask containing a magnetic stir bar, gas inlet adapter, and dry ice/acetone cooled gas condenser was filled with 2.0 g (13 mol) of 3-chloro-2,2,3-trifluoropropionitrile (**9**). Excess liquid ammonia was condensed into the flask which was cooled in dry ice/acetone cold bath. The cold bath was removed, and the solution was stirred under reflux for 30 min. The dry ice cooled gas condenser was removed, and the excess liquid ammonia was allowed to evaporate at room temperature. After the ammonia had evaporated, the remaining volatiles were removed under vacuum (0.1 mmHg) at room temperature to leave amidine as an oil. A 5 L three-necked flask was fitted with a 500 mL pressure equalizing dropping funnel containing a solution of 40 g (0.39 mol) of NaBr dissolved in 180 mL of 12% sodium hypochlorite, a large magnetic stir bar, and a vacuum adapter. The flask was filled with 8.0 g (0.09 mol) of dry LiBr and 80 mL of dry DMSO. Once the solid had dissolved, the amidine was dissolved in a few milliliters of DMSO and added to the flask. A glass stopper was added to the third neck of the flask. The vacuum adapter was connected through a series of three traps maintained at -40 °C, -78 °C, and -196 °C to a mechanical vacuum pump, and the pump was started. Once the pressure of the system reached 0.1 Torr, the stir bar was started and the sodium hypobromite solution was added to the flask over the course of about 1 min. The products were continuously pumped through the train of traps for the next 20 min and then the reaction was stopped. The -78 °C trap was allowed to warm to room temperature, and the product was separated from the water to give 30% yield of product as a clear liquid. Final purification used preparative GLC. ^1H NMR: δ 6.42 (multiplet). ^{19}F NMR: δ -113.0 (ddd, $J_{\text{F-F}} = 15.0$ Hz, $J_{\text{F-F}} = 32.0$ Hz, $J_{\text{F-H}} = 6.6$ Hz), -155.7 (dt, $J_{\text{F-F}} = 15.0$ Hz, $J_{\text{F-F}} = 15.0$ Hz, $J_{\text{F-H}} = 48.0$ Hz).

Preparation of 3-Fluoro-3-(2-chloro-1,1,2-trifluoroethyl)-3*H*-diazirine (5**).** A solution of 0.5 g (2.6 mmol) of 3-bromo-3-(2-chloro-1,1,2-trifluoroethyl)-3*H*-diazirine, 5.0 mL of 1,2-dichlorobenzene, and 5.0 mL of a 1.0 M solution of tetrabutylammonium fluoride in tetrahydrofuran which had been evaporated was stirred for 24 h at 0 °C. The volatile product was vacuum fractionated through a series of two U-traps (-30 °C, -78 °C) and the product collected in the last trap to give a

20% yield of product as an extremely volatile liquid. ^1H NMR: δ 6.50 (ddd, 1H, $J_{\text{H-F}} = 6.0$ Hz, $J_{\text{H-F}} = 7.5$ Hz, $J_{\text{H-F}} = 48.0$ Hz). ^{19}F NMR: δ -121.8 (2F, m), -158.3 (1F, m), -170 (1F, m).

Preparation of 1,2-Dibromo-2-chloro-1,1-difluoroethane (12**).** To a 250 mL rb two-necked flask containing a stir bar was added 50 g (0.77 mol) of zinc dust and 75 mL of 1,4-dioxane distilled over sodium. To one neck, a 50 mL addition funnel containing 94 g (0.48 mol) of 1-bromo-1-chloro-2,2,2-trifluoroethane (halothane) was added, and to the other an ice-cooled condenser, connected by means of Tygon tubing to a 250 mL long-neck rb flask cooled in a -78 °C dry ice/acetone bath, was positioned. The Zn dust/dioxane slurry was heated in a 95-100 °C oil bath. To this heated mixture was added halothane dropwise over the course of 3 h. The temperature of the oil bath never rose above 100 °C. Upon completion of the halothane addition, the reaction mixture was heated for another hour. The contents of the longneck flask were allowed to warm and undergo a static evaporative transfer into another 250 mL longneck rb flask that had been cooled to -78 °C. The mass of transferred 1-bromo-1-chloro-2,2-difluoroethane was 40 g (0.39 mol). A Claisen adapter was attached to the flask. One neck was fitted with a dry ice/acetone cooled condenser, and the other was fitted with a 50 mL addition funnel containing 63 g (0.39 mol) of bromine. Bromine was added in 1 mL increments and resulted in vigorous reflux of the reaction solution. Bromine addition was continued until the solution retained a yellowish color. Atmospheric distillation yielded 82 g (0.31 mol) of clear, colorless product (69% yield, bp = 115 °C). ^1H NMR: δ 5.9 (dd, 1H, $J_{\text{H-F}} = 5.7$ Hz, $J_{\text{H-F}} = 8.5$ Hz). ^{13}C NMR: δ 58 (t, $J_{\text{C-F}} = 32.5$ Hz, CHBrCl), 118 (t, $J_{\text{C-F}} = 308.8$ Hz, CF₂Br). ^{19}F NMR: δ -80 (q_{AB}, $J_{\text{F-F}} = 160$ Hz, $J_{\text{F-H}} = 8.5$ Hz, $J_{\text{F-H}} = 5.8$ Hz).

Preparation of 3-Bromo-3-chloro-2,2-difluoropropionimidic Acid Methyl Ester (13**).** A 100 mL rb flask with a stir bar was filled with 3.5 g (0.053 mol) of KCN and 4 mL of water and 8 mL of methanol. While the reaction mixture was heated in an oil bath at 35 °C, 10 g (0.039 mol) of 1,2-dibromo-2-chloro-1,1-difluoroethane was added dropwise through a water-cooled condenser over the course of 5 min. Upon completion of addition, the mixture was heated and stirred at 50 °C for 2 h. After cooling to room temperature, the reaction mixture is added to 70 mL water. This mixture is extracted with two 25 mL portions of dichloromethane. The organic extracts are dried over Na₂SO₄ and evaporated. Short-path distillation under aspirator pressure resulted in 6.5 g (0.027 mol, 70% yield) of clear, colorless product. BP₅ = 52-54 °C. ^1H NMR: δ 8.3 (broad s, 1H), 5.9 (t, 1H, $J_{\text{H-F}} = 10$ Hz), 3.9 (s, 3H). ^{13}C NMR: δ 54 (t, $J_{\text{C-F}} = 32.6$ Hz), 55 (s), 111 (t, $J_{\text{C-F}} = 252$ Hz), 161 (t, $J_{\text{C-F}} = 32$ Hz). ^{19}F NMR: δ -110 (q_{AB}, 2F, $J_{\text{F-F}} = 249.6$ Hz, $J_{\text{F-H}} = 9.9$ Hz). Anal. (C₄H₅BrClF₂NO): C, H, N.

Preparation of 3-Bromo-3-chloro-2,2-difluoropropionimidic Acid Methyl Ester (14**).** To an ice-cooled flask containing 11 g (0.046 mol) of 3-bromo-3-chloro-2,2-difluoropropionimidic acid methyl ester was added with stirring 10 mL (0.27 mol) of concentrated HCl over the course of 20 min. Upon completion of the addition, the solution was stirred for an additional 15 min. This solution was extracted with three 50 mL portions of diethyl ether. The combined ether layers were dried over Na₂SO₄ and evaporated. Short-path distillation under aspirator pressure yielded 8.75 g (0.036 mol, 75% yield) of clear, colorless product. BP₈ = 53-55 °C. ^1H NMR: δ 5.9 (t, 1H, $J_{\text{H-F}} = 10$ Hz), 3.9 (s, 3H). ^{13}C NMR: δ 53 (t, $J_{\text{C-F}} = 31$ Hz), 54 (s), 111 (t, $J_{\text{C-F}} = 255$ Hz), 161 (t, $J_{\text{C-F}} = 31$ Hz). ^{19}F NMR: δ -110 (q_{AB}, 2F, $J_{\text{F-F}} = 254.6$ Hz, $J_{\text{F-H}} = 9.8$ Hz). Anal. (C₄H₄BrClF₂O₂): C, H.

Preparation of (3-Bromo-3-chloro-2,2-difluoropropylidene)-*tert*-butyl Amine (15**).** A solution of 20.0 g (0.083 mol) of 3-bromo-3-chloro-2,2-difluoropropionimidic acid methyl ester and 100 mL of anhydrous ether is cooled with stirring to -78 °C under a nitrogen atmosphere. A solution of 68 mL (0.1 mol) of a 1.5 M solution of DIBAL-H in toluene was added dropwise via syringe over the course of 20 min. The mixture was stirred at -78 °C for 2 h and was allowed to warm and stir at 0 °C for 30 min. After it was recooled back to -78 °C, the mixture was

quenched with 3 mL of methanol. The mixture was added to 200 mL of 0.5 N HCl, and the solution was extracted with three portions of ether. The combined ether layers were washed with aqueous 0.5 N HCl solution, saturated NaHCO₃, and brine. The organic layer was dried over Na₂SO₄ and evaporated. Toluene (40 mL) was added to the oil, and the resulting solution was brought to reflux for 2 h. After the solution had cooled, the water layer was removed. *tert*-butyl amine (22 mL, 0.20 mol) was added, and the resulting solution was again brought to reflux 1.5 h. After cooling, the solution was dried over Na₂SO₄ and evaporated. Short-path distillation under aspirator pressure yielded 15.1 g (0.057 mol, 67% yield) of clear, colorless product. BP₂₅ = 90 °C. ¹H NMR: δ 7.6 (t, 1H, *J*_{H-F} = 3.5 Hz), 6.0 (t, 1H, *J*_{H-F} = 9.9 Hz), 1.2 (s, 9H). ¹³C NMR: δ 29 (s), 55 (t, *J*_{C-F} = 33.1 Hz), 59 (s), 114 (t, *J*_{C-F} = 249 Hz), 149 (t, *J*_{C-F} = 33.3 Hz); ¹⁹F NMR: δ -106 (q_{AB}, 2F, *J*_{F-F} = 258 Hz, *J*_{F-H} = 9.8 Hz, *J*_{F-H} = 3.4 Hz). Anal. (C₇H₁₁BrClF₂N): C, H, N.

Preparation of (2-Bromo,2-chloro-1,1-difluoroethyl)-1-*tert*-butyl-diaziridine (16). A 25 mL rb flask containing a stir bar was filled with 1.0 g (0.0038 mol) of 3-bromo-3-chloro-2,2-difluoropropylidene)-*tert*-butyl amine, 4 mL of anhydrous ethanol, and 2 mL of triethylamine. The solution was cooled to 0 °C and 0.88 g (0.007 mol) of hydroxylamine-*O*-sulfonic acid was added. After the mixture had stirred for 2 h at 0 °C, 50 mL of ether was added. The resulting solution was washed with three 10 mL portions of water. The organic layer was dried (Na₂SO₄) and evaporated to leave 0.58 g (0.0021 mol, 55% yield) of product that was solid below room temperature but turned to an oil at room temperature. ¹H NMR: δ 5.9 (t, 1H, *J*_{H-F} = 3.6 Hz), 5.8 (t, 1H, *J*_{H-F} = 3.4 Hz), 3.4 (multiplet, 1H), 2.3 (broad s, 1H), 1.1 (ds, 9H). ¹³C NMR: δ 26 (s), 55 (t, *J*_{C-F} = 35 Hz), 51 (q, *J*_{C-F} = 32.4 Hz), 60, 115 (t, *J*_{C-F} = 246 Hz). ¹⁹F NMR: δ -115, -116 (dq_{AB}, 2F, *J*_{F-F} = 245 Hz, *J*_{F-H} = 5.2 Hz). Anal. (C₇H₁₂BrClF₂N₂): C, H, N.

Preparation of 3-(2-Bromo-2-chloro-1,1-difluoroethyl)-3H-diazirine (4). A 50 mL rb flask with a stir bar was filled with 2.0 g (0.0073 mol) of 2-bromo,2-chloro-1,1-difluoroethyl)-1-*tert*-butyl-diaziridine, 40 mL of methylene chloride, and 1.56 g (0.009 mol) of NBS (*N*-bromosuccinimide). The flask was covered with tin foil and was stirred for 1.5–2.0 h at room temperature. A flow of nitrogen gas was used to evaporate most of the solvent. When approximately 5 mL remained, the volatiles were fractionated under vacuum (0.01 Torr) through a series of three U-traps cooled to -10 °C, -45 °C, and -78 °C. The contents of the -45 °C U-trap were further purified by preparative gas chromatography (10 ft, 20% SF-96) to give 0.355 g (0.0016 mol, 23% yield) of 5 as a colorless oil. BP: >110 °C (decomposition). ¹H NMR: δ 5.8 (t, 1H, *J*_{H-F} = 7.3 Hz), 1.7 (t, 1H, *J*_{H-F} = 7.4 Hz). ¹³C NMR: δ 19.6 (t, *J*_{C-F} = 32.6 Hz), 54.2 (t, *J*_{C-F} = 36.4 Hz), 114.4 (t, *J*_{C-F} = 251.5 Hz). ¹⁹F NMR: δ -106.8 (dt, 2F, *J*_{F-F} = 24 Hz, *J*_{F-H} = 7.3 Hz).

Preparation of 1-Azido-2-bromo-2-chloro-1,1-difluoroethane (6). To a mixture of 10.0 g (0.154 mol) of sodium azide in 200 mL of methylene chloride was added 10 mL of concentrated HCl and 3 mL of water. The mixture was vigorously stirred for 10 min, then 6.0 g (0.038 mol) of bromine was added in one portion. After the mixture was stirred for an additional 30 min, the organic layer was separated and was added to a 500 mL rb flask equipped with a dry ice cooled gas condenser and magnetic stir bar. 1-Bromo-1-chloro-2,2-difluoroethane (4.8 g, 0.027 mol) was condensed into the flask, and the flask was irradiated with a 200 W sodium lamp for 4 h under a dry ice gas condenser. The methylene chloride was removed by distillation through a Vigreux column and the product was distilled to yield 80% of a clear, colorless oil, bp 123 °C. IR: 2250 cm⁻¹. ¹H NMR: δ 5.71 (t, *J*_{H-F} = 5.9 Hz). ¹³C NMR: δ 55.0 (t, *J*_{C-F} = 39.6 Hz), 119.0 (t, *J*_{C-F} = 70.0 Hz). ¹⁹F NMR: δ -81.5 (m).

Fluorescence Spectroscopy. Several of the designed compounds contain heavy atoms or delocalized electrons that can quench tryptophan fluorescence if bound in the immediate vicinity (<5 Å).² Thus, to determine if the various inhaled anesthetics can gain access to and exhibit selectivity for the

tryptophan-containing regions of bovine serum albumin, increasing concentrations of these compounds (from stock buffer solutions) were added to 4 mL fluorescence cuvettes containing ~2 μM protein and examined in a Shimadzu RF 5301 PC spectrofluorophotometer (Shimadzu Scientific Instruments, MD) using 295 nm excitation and emission scanning. Care was taken to eliminate all air from the cuvette with the last addition, and spectra were collected at room temperature. Fluorescence values were corrected for inner filter effects due to these compounds as previously published.²

Hydrogen–Tritium Exchange. We have previously shown that stabilization of serum albumin correlates well with anesthetic potency in a series of volatile compounds.²⁷ Amide hydrogen–tritium exchange was used to measure the effect of these compounds on bovine serum albumin stability. For these measurements, protein solutions (10 mg/mL) were incubated with ~5 mCi ³HOH in 1 M GdnCl, 0.1 M NaH₂PO₄ pH 8.5 buffer for at least 18 h at room temperature. The GdnCl increased exposure of protected hydrogens to solvent, and the elevated pH increased the rate of chemical hydrogen exchange—both conditions intended to ensure equilibration of all exchangeable hydrogens in the protein prior to initiation of exchange-out. Free ³HOH was removed and the buffer exchanged with a PD-10 gel filtration column (Sigma, MO), and exchange-out was thereby initiated. After recovery from the column, the protein solution was immediately transferred to pre-filled Hamilton (Reno, NV) gas-tight syringes containing the photolabels and equipped with repeaters (see figure legends). Aliquots were precipitated with 2 mL of ice-cold 10% trichloroacetic acid at timed intervals over at least 6 h. The precipitated protein was rapidly vacuum filtered through Whatman GF/B filters and washed with 8 mL of ice-cold 2% TCA. ³H retained by the protein was determined by liquid scintillation counting as above. Protection factor ratios (PFRs) were determined by dividing the time required for a given hydrogen to exchange under the different conditions for the last three to five hydrogens in common for the two conditions, and ΔΔ*G* was determined using the equation ΔΔ*G* = *RT* ln(PFR).

Oocyte Electrophysiology. (i) Preparation of cRNA from cDNA. GABA_A receptor cDNA sequences cloned into plasmid vectors were used to synthesize capped RNA transcripts for expression in oocytes. Phage polymerases (T7, SP6, or T3) were used to make full-length capped RNA transcripts from linearized template DNA using a commercially available kit (mMessage mMachin (Ambion)) according to manufacturer's protocol.

(ii) Injection of Xenopus Oocytes and Voltage-Clamp Recording. Oocytes were obtained from adult female *Xenopus* as described before.²⁸ Ovarian lobes were opened with forceps, and the follicular layer was softened by incubation with collagenase in OR2 solution (82.5 mM NaCl, 2 mM KCl, 1 mM MgCl₂, 5 mM HEPES, pH 7.5). Remaining follicular cells were manually removed, and the oocytes were washed and placed in ND96 medium (96 mM NaCl, 2 mM KCl, 1 mM MgCl₂, 1.8 mM CaCl₂, 5 mM HEPES, 5 mM pyruvate, pH 7.5). Stage V–VI oocytes were injected in the vegetal pole with RNA (50 nL; 1–2 ng of each cRNA transcript). For expression of these heteromeric receptors, subunit cRNAs were injected in 1:1 ratio. Oocytes were maintained at 18 °C in ND96 with antibiotic (50 μg/mL gentamicin) for 3–5 days before use in experiments.

For recording, oocytes were positioned in a small Perspex chamber and continuously superfused (5 mL/min) with ND96 solution. Oocytes were impaled with borosilicate glass microelectrodes filled with 3 M KCl (resistance 0.5–3 MΩ), and currents were recorded from oocytes using a two-electrode voltage-clamp amplifier (GeneClamp 500, Axon Instruments). To record currents, signals were low-pass filtered and digitized, using an A/D interface (MacLab 4/S with chart and scope software, A.D. Instruments, Mountain View, CA), and stored on the hard disk of a computer for offline analysis.

All compounds were solubilized in GABA-containing oocyte buffer as above, loaded into gas-tight Hamilton syringes, and

applied by syringe pump superfusion. Control GABA currents were also obtained by syringe pump superfusion, while a gravity system was used for washout superfusion.

Photolabeling. Small aliquots of pH 7 phosphate buffer containing ~1 mg/mL HSA domain II (a kind gift from R. Bahgavan, University of Hawaii) and 2 mM of compound 4 were placed in a 1 mm path length quartz cuvette and exposed to 300 nm light (broad emission from 280 to 320 nm) at 2 mm distance for 5 min. For comparison, peptide was also exposed to 5 mM halothane and 1 min of 254 nm light. The solutions were washed using 3 kDa cutoff Microcon filters (Amicon) to remove soluble photolysis products and salts, then lyophilized, and resuspended in 0.1% TFA. Small aliquots were examined with MALDI-MS for a shift in peptide MW that would indicate covalent incorporation of the adduct.

Tadpole Studies. Xenopus tadpoles were used to examine anesthetic activity of the compounds in a semiquantitative fashion. About 10 tadpoles were placed in 20 mL glass vials containing pond water and increasing concentrations of the compounds, presolubilized by vigorous shaking/sonication of pond water with aliquots of neat compound. Tadpoles were observed for loss-of-righting reflex for 5 min, then immediately transferred into large containers of fresh pond water, and carefully observed for recovery. The tadpoles were then observed intermittently for 3 h. Control experiments verified an absence of effect of the manipulations on tadpole activity. The potency values derived are considered estimates and within 2-fold of the real value. We verified this by reproducing the expected EC₅₀ for halothane of about 0.25 mM.

Solubility. Octanol–water partition coefficients were determined as follows. The diazo compound 1 has a characteristic absorbance at ~400 nm, and the diazirine compounds absorb between 300 and 350 nm. Thus, compounds were solubilized in water and then loaded into 10 mL gas-tight Hamilton syringes. Absorbance of an aliquot was recorded, and then exactly 1 mL of octanol was drawn into the syringe and mixed by rotation for an hour. The octanol–water mixture was allowed to completely separate for another hour, and then absorbance of the water phase was measured again. Molar partition was calculated by multiplying the difference in water absorbance by the ratio of water to octanol volume and dividing by the ending water absorbance. This simple method reproduced the published value for halothane to within 10%.

References

- (1) Eckenhoff, R. G.; Johansson, J. S. Molecular interactions between inhaled anesthetics and proteins. *Pharmacol. Rev.* **1997**, *49*, 343–367.
- (2) Johansson, J. S.; Eckenhoff, R. G.; Dutton, P. L. Binding of halothane to serum albumin demonstrated using tryptophan fluorescence. *Anesthesiology* **1995**, *83*, 316–324.
- (3) Eckenhoff, R. G.; Tanner, J. W.; Liebman, P. A. Cooperative binding of inhaled anesthetics and nucleotide to firefly luciferase. *PROTEINS: Struct., Funct. Genet.* **2001**, *42*, 436–441.
- (4) Eckenhoff, R. G.; Pidikiti, R.; Reddy, K. S. Anesthetic stabilization of protein intermediates: Myoglobin and halothane. *Biochemistry* **2001**, *40*, 10819–10824.
- (5) Dubois, B. W.; Evers, A. S.¹⁹F-NMR spin–spin relaxation (T₂) method for characterizing anesthetic binding to proteins: analysis of isoflurane binding to albumin. *Biochemistry* **1992**, *31*, 7069–7076.
- (6) Ueda, I.; Yamanaka, M. Titration calorimetry of anesthetic–protein interaction: Negative enthalpy of binding and anesthetic potency. *Biophys. J.* **1997**, *72*, 1812–1817.
- (7) Eckenhoff, R. G.; Tanner, J. W. Differential halothane binding and effects on serum albumin and myoglobin. *Biophys. J.* **1998**, *75*, 477–483.
- (8) Eckenhoff, R. G.; Shuman, H. Halothane binding to soluble proteins determined by photoaffinity labeling. *Anesthesiology* **1993**, *79*, 96–106.
- (9) Eckenhoff, R. G. Amino acid resolution of halothane binding sites in serum albumin. *J. Biol. Chem.* **1996**, *271*, 15521–15526.
- (10) Eckenhoff, M. F.; Eckenhoff, R. G. Quantitative autoradiography of halothane binding in rat brain. *J. Pharmacol. Exp. Therap.* **1998**, *285*, 371–376.
- (11) Eckenhoff, M. F.; Eckenhoff, R. G. γ -Aminobutyric acid enhancement of halothane binding in rat cerebellum. *Neurosci. Lett.* **2000**, *286*, 111–114.
- (12) For a recent review see, Brahm, D. L. S.; Dailey, W. P. Fluorinated Carbenes. *Chem. Rev.* **1996**, *96*, 1585–1632.
- (13) Bhattacharya, A. A.; Curry, S.; Franks, N. P. Binding of the general anesthetics propofol and halothane to human serum albumin. *J. Biol. Chem.* **2000**, *275*, 38731–38738.
- (14) Harris, R. A.; Mihic, S. J.; Dildy-Mayfield, J. E.; Machu, T. K. Actions of anesthetics on ligand-gated ion channels: Role of receptor subunit composition. *FASEB J.* **1995**, *9*, 1454–1462.
- (15) Mihic, S. J.; Ye, Q.; Wick, M. J.; Koltchine, V. V.; Krasowski, M. D.; Finn, S. E.; Mascia, M. P.; Valenzuela, C. F.; Hanson, K. K.; Greenblatt, E. P.; Harris, R. A.; Harrison, N. L. Sites of alcohol and volatile anesthetic action on GABA_A and glycine receptors. *Nature* **1997**, *389*, 385–389.
- (16) Atherton, J. H.; Fields, R. Reactions of trifluoromethylcarbene with cis- and trans-2-butenes. *J. Chem. Soc. (C)* **1967**, 1450–1454.
- (17) Dailey, W. P. 3-Fluoro-3-trifluoromethyl-diazirine. *Tetrahedron Lett.* **1987**, *47*, 5801–5804.
- (18) England, D. C.; Melby, L. R. 3-Chloro-2,2,2-trifluoropropionic acid. *Org. Synth.* **1973**, *Coll. Vol. V*, 239–242.
- (19) Jakubowitsch, A. Ya.; Sergeev, A. P. Preparation of polyfluoro acids and their derivatives from polyfluoroolefins and hydrocyanic acid. *Chem. Abstr.* **1960**, *54*, 86615i.
- (20) Graham, W. H. The halogenation of amidines. I. Synthesis of 3-halo- and other negatively charged diazirines. *J. Am. Chem. Soc.* **1965**, *87*, 4396–4397.
- (21) Cox, D. P.; Moss, R. A.; Terpinski, J. Exchange reactions of halodiazirines. Synthesis of fluorodiazirines. *J. Am. Chem. Soc.* **1983**, *105*, 6513–6514.
- (22) Hudlicky, M.; Lejhancova, I. Organic compounds of fluorine. VIII. Reactions of fluorohaloethanes. *Czech. Coll. Chem. Comm.* **1965**, *30*, 2491–2493.
- (23) Erni, B.; Khorana, H. G. Fatty Acids containing photoactivable carbene precursors. Synthesis and photochemical properties of 3,3-bis(1,1-difluoroethyl)diazirine and 3-(1,1-difluoroethyl)-3H-diazirine. *J. Am. Chem. Soc.* **1980**, *102*, 3888–3896.
- (24) Hassner, A.; Boerwinkle, F. P.; Levy, A. B. Stereochemistry of halogen azide additions to olefins. The stability of three-membered iodonium vs bromonium ions. *J. Am. Chem. Soc.* **1970**, *92*, 4879–4883.
- (25) Frisch, M. J.; Trucks, G. W.; Schlegel, H. B.; Gill, P. M. W.; Johnson, B. G.; Robb, M. A.; Cheeseman, J. R.; Keith, T.; Petersson, G. A.; Montgomery, J. A.; Raghavachari, K.; Al-Laham, M. A.; Zakrzewski, V. G.; Ortiz, J. V.; Foresman, J. B.; Cioslowski, J.; Stefanov, B. B.; Nanayakkara, A.; Challacombe, M.; Peng, C. Y.; Ayala, P. Y.; Chen, W.; Wong, M. W.; Andres, J. L.; Replogle, E. S.; Gomperts, R.; Martin, R. L.; Fox, D. J.; Binkley, J. S.; Defrees, D. J.; Baker, J.; Stewart, J. P.; Head-Gordon, M.; Gonzalez, C.; Pople, J. A. *Gaussian 94*, revision C.3; Gaussian, Inc.: Pittsburgh, PA, 1995.
- (26) Tang, P.; Zubryzcki, I.; Xu, Y. Ab Initio Calculation of Structures and Properties of Halogenated General Anesthetics: Halothane and Sevoflurane. *J. Comput. Chem.* **2001**, *22*, 436–444.
- (27) Eckenhoff, R. G. Do specific or nonspecific interactions with protein underlie inhaled anesthetic action? *Mol. Pharmacol.* **1998**, *54*, 610–615.
- (28) Greenblatt, E. P.; Meng, X. Divergence of volatile anesthetic effects in inhibitory neurotransmitter receptors. *Anesthesiology* **2001**, *94*, 1026–1033.

JM0104926